ACS APPLIED MATERIALS & INTERFACES

Research Article

www.acsami.org

Application of Biuret, Dicyandiamide, or Urea as a Cathode Buffer Layer toward the Efficiency Enhancement of Polymer Solar Cells

Xuemei Zhao,[†] Chenhui Xu,[†] Haitao Wang,[†] Fei Chen,[‡] Wenfeng Zhang,[†] Zhiqiang Zhao,[†] Liwei Chen,[‡] and Shangfeng Yang*[,†]

[†]Hefei National Laboratory for Physical Sciences at Microscale, CAS Key Laboratory of Materials for Energy Conversion & Department of Materials Science and Engineering, University of Science and Technology of China (USTC), Hefei 230026, China

[‡]i-LAB, Suzhou Institute of Nano-Tech and Nano-Bionics, Chinese Academy of Sciences, Suzhou 215123, China

Supporting Information

ABSTRACT: Three amino-containing small-molecule organic materials—biuret, dicyandiamide (DCDA), and urea—were successfully applied as novel cathode buffer layers (CBLs) in P3HT:PCBM bulk heterojunction polymer solar cells (BHJ-PSCs) for the first time, resulting in obvious efficiency enhancement. Under the optimized condition, the power conversion efficiencies (PCEs) of the CBL-incorporated BHJ-PSC devices are 3.84%, 4.25%, and 4.39% for biuret, DCDA, and urea, which are enhanced by ∼15%, ∼27%, and ∼31%, respectively, compared to the reference poly(3-hexylthiophene-2,5-diyl) : [6,6]-phenyl-C_{61}-butyric acid methyl ester (P3HT:PCBM) BHJ-PSC device without any CBL. The efficiency enhancement is primarily attributed to the increases of both short-circuit current density (J_{sc}) and fill factor (FF), for which the enhancement ratio is found to be sensitively dependent on the molecular structure of small-molecule organic materials. The surface morphologies and surface potential changes of the CBL-incorporated P3HT:PCBM photoactive layers were studied by atomic force microscopy and scanning Kelvin probe microscopy, respectively, suggesting the formation of an interfacial dipole layer between the photoactive layer and Al cathode, which may decrease the energy level offset between the work function of Al and the lowest unoccipoed molecular orbital level (LUMO) of the PCBM acceptor and consequently facilitate electron extraction by the Al cathode. The difference in the enhancement effect of biuret, DCDA, and urea is due to their difference on the work function matching with P3HT:PCBM. Besides, the coordination interaction between the lone-pair electrons on the N atoms of the amino ($-NH_2$) group and the Al atoms may prohibit interaction between Al and the thiophene rings of P3HT, contributing to the efficiency enhancement of the CBL-incorporated devices as well. In this sense, the different CBL performance of biuret, DCDA, and urea is also proposed to partially originate from the differences on their chemical structure, specifically the number of amino groups.

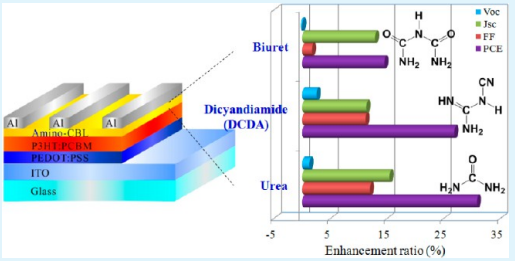

KEYWORDS: *polymer solar cells, biuret, dicyandiamide, urea, amino group, cathode buffer layer*

INTRODUCTION

Polymer solar cells (PSCs) have been attracting considerable attention as promising renewable energy sources owing to their unique advantages of light-weight, low-cost, high-flexibility, and easy roll-to-roll fabrication.[1−9] Until now, a bulk heterojunction (BHJ) structure has been popularly used as the most efficient configuration of PSCs, for which an interpenetrating network of a conjugated polymer donor like poly(3-hexylthiophene-2,5-diyl) (P3HT) and a soluble fullerene acceptor material such as [6,6]phenyl-C_{61}-butyric acid methyl ester (PCBM) exists in the photoactive layer.[10,11] Owing to the recent advances in the synthesis of novel polymer donors, nanoscale morphology control, and device structure optimization, a power conversion efficiency (PCE) approaching 10% has been achieved for solution-processable state-of-the-art BHJ-PSCs, which needs to be improved further to meet the requirement for commercial applications.[12−14] Optimization of the device structure, particularly the interfaces between donor (acceptor)/electrodes, has been demonstrated to be so crucial that such interfaces play a determinative role in efficient charge transport and extraction.[12−21]

For the extensively studied P3HT:PCBM BHJ-PSCs, it is well-known that there is an energy level offset of ca. 0.3 eV between the work function of Al (4.3 eV) and the lowest unoccupied molecular level (LUMO) level of the PCBM acceptor (4.0 eV), resulting in unfavorable electron extraction due to charge accumulation and consequently a recombination loss of charge carriers.[10,11,17−22] Therefore, to decrease such an energy level offset is of high importance for optimization of the electrical contact between the active layer and cathode.[23−26] Cathode buffer layers (CBLs) thus introduced between the active layer and cathode have been extensively investigated

Received: January 2, 2014
Accepted: February 27, 2014
Published: February 27, 2014

recently and demonstrated to improve the cathode efficiency in collecting and extracting electrons, and this is typically fulfilled by inducing interfacial charge redistribution, geometry modifications, and/or chemical reactions.[17−21] Following the pioneering work applying the low work function metal Ca as an efficient CBL, which, however, suffers from poor stability because the thermally deposited Ca buffer layer is quite reactive,[27] up to now the reported CBL materials have been extended to other low-work-function metals such as Ba,[23] alkali-metal compounds such as LiF,[28,29] metal oxides such as TiO_x,[30,31] and organic materials including surfactants,[32] conjugated or nonconjugated polymers,[33,34] and small molecules.[25,35−39] Among them, the latter approach is more facile because the incorporation of organic materials can be accomplished by solution processing. In particular, small-molecule organic material is more readily available than polymers and advantageous in terms of its certain molecular weight and assembly structure. So far, few studies on using small-molecule organic materials as CBLs have been reported. For instance, Deng et al. studied the effect of several small-molecule electron-transporting materials, 2-(4-biphenyl)-5-(4-*tert*-butylphenyl)-1,3,4-oxidiazole (PBD), tris(8-hydroxyquinolinato)aluminum (Alq_3), and bis[2-(2-benzothiazoly)-phenolato]zinc(II) [$Zn(BTZ)_2$], which were incorporated via thermal evaporation, on the performance of P3HT:PCBM PSCs and found that the insertion of electron-transporting layers improved the open-circuit voltage (V_{oc}) and PCE owing to the increased built-in potential at the interface between the photovoltaic active layer and Al electrode.[35] Ma et al. synthesized a new alcohol-soluble electron-transporting material, 4,7-diphenyl-1,10-phenanthroline-2,9-dicarboxylic acid (DPPA), which was used to modify ZnO, and then incorporated it into inverted P3HT:PCBM PSCs as the electron-transporting layer, resulting in an enhancement of about 10% compared with the device without DPPA. Moreover, DPPA was also used as the sole electron-extracting layer, affording PCE enhancement as well because of the improved interfacial contact between the substrate and active layer.[25] Li et al. applied a solution-processable titanium chelate, titanium diisopropoxide bis(2,4-pentanedionate) (TIPD), as the CBL in both normal-structure poly[2-methoxy-5-(2′-ethylhexyloxy)-1,4-phenylenevinylene] (MEH-PPV):PCBM and inverted-structure poly[4,8-bis(alkyloxy)benzo[1,2-*b*:4,5-*b*′]dithiophene-2,6-diyl-*alt*-(alkylthieno[3,4-*b*]thiophene-2-carboxylate)-2,6-diyl] (PBDTTT-C):$PC_{71}BM$ PSCs, achieving PCE enhancement of 51.8% and 16%, respectively.[36,37] More recently, the same group developed several new functionalized fullerene derivatives, namely, [6,6]phenyl-C_{61}-butyric acid 2-[[2-(dimethylamino)ethyl](methyl)amino]ethyl ester (PCBDAN), [6,6]phenyl-C_{61}-butyric acid 2-[[2-(trimethylammonium)ethyl](dimethyl)ammonium] ethyl ester diiodonium (PCBDANI), and an amine group functionalized fullerene derivative DMAPA-C_{60}, as CBLs being universally applicable in PSCs based on different photoactive layers and thus promising in replacing the unstable Ca buffer layer in PSCs.[38,39]

Herein, we report for the first time the application of several small-molecule organic materials containing amino ($-NH_2$) groups as novel CBLs in P3HT:PCBM BHJ-PSCs, leading to obvious efficiency enhancement. Three amino-containing small-molecule organic materials with different numbers and bonding environments of the amino groups, including biuret, dicyandiamide (DCDA), and urea, were studied, and their effect toward the efficiency enhancement of PSCs was compared, revealing the role of the amino group on the performance of these small-molecule organic compounds as CBLs.

EXPERIMENTAL SECTION

Materials. The indium tin oxide (ITO) glass substrate with a sheet resistance of 8 Ω $\square^{-1}$ was purchased from Shenzhen Nan Bo Group, China. Poly(3,4-ethylenedioxythiophene):poly(styrene sulfonate) (PEDOT:PSS; Baytron P) was purchased from SCM Industrial Chemical Co., Ltd. P3HT and PCBM were bought from Luminescence Techology Corp. and Nichem Fine Technology Co., Ltd., respectively. Biuret ($C_2H_5N_3O_2$, ≥99.0%), dicyandiamide (DCDA; $C_2H_4N_4$, ≥98.0%), and urea (CH_4N_2O, ≥99.0%) were purchased from Sinopharm Chemical Reagent Co., Ltd. All chemicals were used as received without further purification.

Device Fabrication. Our detailed fabrication procedure of the P3HT:PCBM BHJ-PSCs has been reported previously.[32,34,40−44] Briefly, a thin film (~35 nm thick) of PEDOT:PSS (Baytron P) was spin-coated onto the cleaned ITO-coated substrate treated by ozone−ultraviolet and then annealed at 120 °C for 30 min. The P3HT:PCBM (1:0.8, w/w) blend was dissolved in chlorobenzene by stirring at 40 °C overnight. This blend solution was spin-coated on top of the PEDOT:PSS film to form a thin active layer (~80 nm thick). Biuret, DCDA, and urea were dissolved in methanol (MeOH) to form different CBL solutions with different concentrations (0.5, 1.0, and 1.5 mg mL^{-1}), which were directly spin-coated on top of the P3HT:PCBM active layers at different spin-coating speeds of 1000, 3000, and 5000 rpm; accordingly, the condition for CBL incorporation was optimized. All of the solution processes were carried out in an air atmosphere. Then the device was transferred into a vacuum chamber (~10^{-5} Torr), and an Al cathode (~100 nm thick) was thermally deposited atop the CBL through a shadow mask to define the active area of the devices (2 × 5 mm^2). Finally, thermal annealing was carried out at 135 °C for 10 min under a nitrogen atmosphere.

Measurements and Characterization. The current density−voltage (J−V) characterization of BHJ-PSCs was carried out by using a Keithley 2400 source measurement unit under simulated AM 1.5 irradiation (100 mW cm^{-2}) with a standard xenon-lamp-based solar simulator (Oriel Sol 3A, USA). The solar simulator illumination intensity was calibrated by a monocrystalline silicon reference cell (Oriel P/N 91150 V, with KG-5 visible color filter) calibrated by the National Renewable Energy Laboratory (NREL). All of the measurements were carried out in air, and a mask with a well-defined area size of 10.0 mm^2 was attached to the cell to define the effective area in order to ensure accurate measurement. More than 10 devices were fabricated and measured independently under each experimental condition to ensure the consistency of the data. The average data were used in the following discussions.

Atomic force microscopy (AFM) measurements were carried out on a Veeco DI-MultiMode V scanning probe microscope in tapping mode. The thickness of the CBL was estimated by a Veeco DI-Innova scanning probe microscope by using a sharp blade to generate ~10-μm-wide cuts in the layer. Scanning Kelvin probe microscopy (SKPM) measurements were performed on a Park XE-120 scanning probe microscope using SKPM mode. Samples were treated by a nitrogen flow for 20 min to remove air prior to the measurement and then measured in a nitrogen atmosphere. A standard HOPG measurement was done as a reference prior to the measurement of each sample in order to avoid the possible variations resulting from the tip and atmosphere.

RESULTS AND DISCUSSION

Optimization of Biuret Incorporation as the CBL and Performance of Biuret-Incorporated P3HT:PCBM BHJ-PSC Devices. It is known that the thickness of the CBL plays an important role in its performance in BHJ-PSCs.[22,23,35,45,46] We first optimized the thickness of the biuret CBL by adjusting

the solution concentration and spin-coating speed of the biuret that was incorporated between the P3HT:PCBM active layer and Al cathode (see Scheme 1). Different biuret solutions in

Scheme 1. Device Architecture of ITO/PEDOT:PSS/P3HT:PCBM/CBL/Al BHJ-PSCs with the Incorporation of Different CBLs (Biuret, DCDA, or Urea) Incorporated via Spin Coating

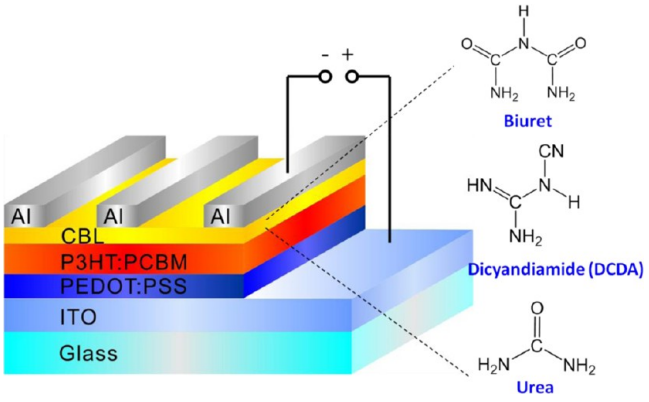

MeOH with concentrations of 0.5, 1.0, and 1.5 mg mL^{-1} were spin-coated on top of the P3HT:PCBM active layers at a fixed spin-coating speed of 3000 rpm. The as-prepared ITO/PEDOT:PSS/P3HT:PCBM/biuret/Al devices are annealed and measured under simulated AM 1.5 irradiation (100 mW cm^{-2}) in an air atmosphere. Figure 1 compares the $J-V$ curves

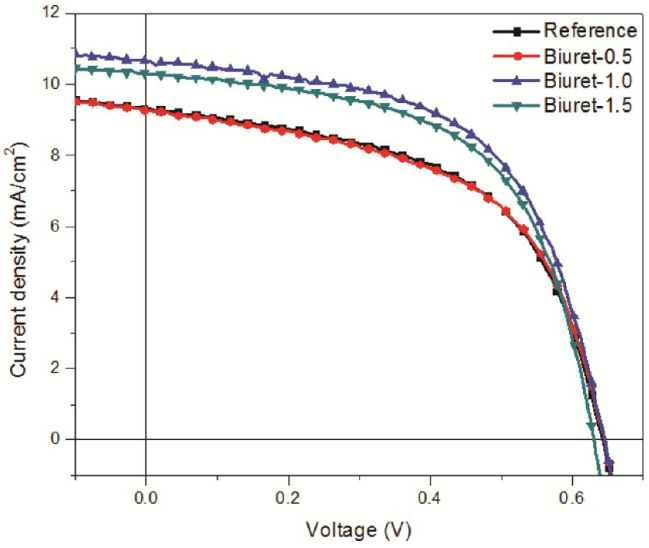

Figure 1. $J-V$ curves of the ITO/PEDOT:PSS/P3HT:PCBM/biuret/Al BHJ-PSCs with a biuret CBL prepared from different concentrations (0.5, 1.0, and 1.5 mg mL^{-1}, denoted as biuret-0.5, biuret-1.0, and biuret-1.5, respectively) and without a biuret buffer layer (reference). The measurements are carried out under AM 1.5 illumination at an irradiation intensity of 100 mW cm^{-2}.

of devices fabricated at different biuret concentrations (abbreviated as biuret-0.5, biuret-1.0, and biuret-1.5), and the measured parameters [short-circuit current (J_{sc}), open-circuit voltage (V_{oc}), fill factor (FF), PCE, series resistance (R_s), and shunt resistance (R_{sh})] based on the average of more than 10 devices fabricated independently under each experimental condition are summarized in Table 1. Compared to the reference ITO/PEDOT:PSS/P3HT:PCBM/Al device (reference) without any CBL, which exhibits a PCE of 3.29%, obviously our biuret-CBL-incorporated devices with relatively high biuret concentrations (biuret-1.0 and biuret-1.5) both exhibit enhancements in PCEs, whereas the device incorporated with a biuret CBL prepared from lower concentration (0.5 mg mL^{-1}, biuret-0.5) shows a PCE comparable to that of the reference device by considering the measurement error. The highest PCE is 3.78% achieved for the device biuret-1.0 prepared from a biuret concentration of 1.0 mg mL^{-1}, which is enhanced by ca. 15% compared to that of the reference P3HT:PCBM device. Upon an increase of the biuret concentration to 1.5 mg mL^{-1}, PCE decreases to 3.49%, which still has a ca. 6% enhancement compared to that of the reference P3HT:PCBM device (see Table 1). Different concentrations of biuret solution spin-coated at the same spin-coating speed resulted in different thicknesses of the biuret; thus, different enhancement performances of a biuret CBL were obtained.

The spin-coating speed is another determinative parameter for the thickness of the film. We next optimize the thickness of a biuret CBL by varying the spin-coating speed (1000, 3000, and 5000 rpm, denoted as biuret-1000, biuret-3000, and biuret-5000, respectively) of a biuret solution with a concentration of 1.0 mg mL^{-1} optimized above, and $J-V$ curves are illustrated in Figure 2. According to the measured photovoltaic parameters (Table 2), all devices incorporated with a biuret CBL exhibit enhanced PCEs compared to the reference P3HT:PCBM device (3.31%). With an increase of the spin-coating speed of the biuret from 1000 to 3000 rpm, PCE of the biuret-incorporated devices increases dramatically (3.45% and 3.72% for biuret-1000 and biuret-3000, respectively), and then PCE decreases to 3.51% with a further increase of the spin-coating speed to 5000 rpm (see Table 2). Accordingly, the optimum spin-coating speed of a biuret CBL is determined to be 3000 rpm, under which the biuret-incorporated device exhibits the maximum PCE of 3.72% with a ca. 13% enhancement compared to that of the reference P3HT:PCBM device.

Performance of P3HT:PCBM BHJ-PSC Devices Incorporated with DCDA and Urea as CBLs. Given that the effect of a biuret as a CBL has been revealed, two other amino-containing small-molecule organic materials, including DCDA and urea, were then used as CBLs as well for a comparative study in order to study the influence of the molecular structure on the performance of these amino-containing compounds as CBLs. Similar optimization experiments were carried out for the cases of using DCDA and urea as CBLs, revealing that the optimum solution concentration (1.0 mg mL^{-1} in MeOH) and spin-coating speed (3000 rpm) for both cases are the same as those for a biuret CBL (see the Supporting Information, section S1). Because biuret, DCDA, and urea CBLs are insulating organic materials, a thicker CBL may block charge transfer from the photoactive layer to the metal cathode, whereas a thinner CBL may not fully cover the surface of the photoactive layer, resulting in direct contact with the Al cathode. Under such optimum conditions, the thicknesses of the biuret, DCDA, and urea films estimated by AFM measurement are ca. 3, 2, and 2 nm, respectively, as discussed further below (see the Supporting Information, Figure S3).

Figure 3 compares the $J-V$ curves of ITO/PEDOT:PSS/P3HT:PCBM/CBL/Al BHJ-PSC devices incorporated with different CBLs including biuret, DCDA, and urea fabricated under identical conditions (curves b–d) and that of the

Table 1. Photovoltaic Parameters of ITO/PEDOT:PSS/P3HT:PCBM/Biuret/Al BHJ-PSCs with Biuret CBLs Prepared from Different Concentrations[a]

device	concn (mg mL^{-1})	V_{oc} (V)	J_{sc} (mA cm^{-2})	FF (%)	PCE (%)	ΔPCE[b] (%)	R_s (Ω cm^2)	R_{sh} (Ω cm^2)
reference		0.64 ± 0.003	9.30 ± 0.21	55 ± 2	3.29 ± 0.14		11.7	380.6
biuret-0.5	0.5	0.64 ± 0.005	9.25 ± 0.13	55 ± 1	3.28 ± 0.11	−0.3	10.9	356.4
biuret-1.0	1.0	0.63 ± 0.005	10.28 ± 0.20	58 ± 1	3.78 ± 0.06	15	9.4	559.1
biuret-1.5	1.5	0.63 ± 0.005	10.26 ± 0.14	54 ± 1	3.49 ± 0.09	6	9.5	293.0

[a]The spin-coating speed is fixed at 3000 rpm. [b]ΔPCE is the enhancement of PCE relative to the reference P3HT:PCBM BHJ-PSCs.

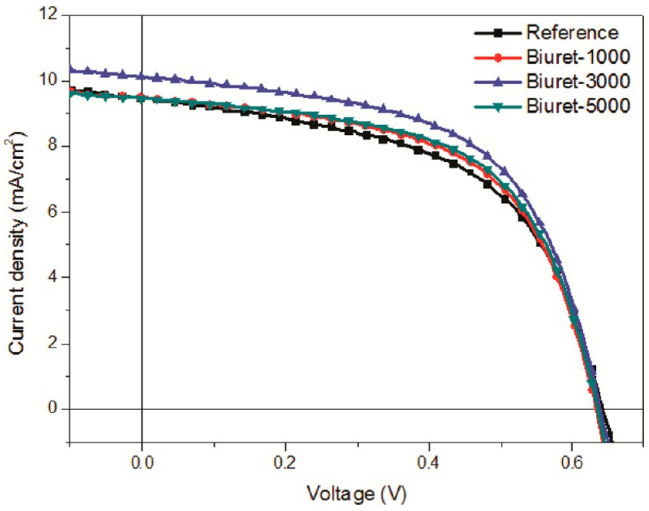

Figure 2. *J*−*V* curves of the ITO/PEDOT:PSS/P3HT:PCBM/biuret/Al BHJ-PSCs with a biuret CBL prepared at different spin-coating speeds (1000, 3000, and 5000 rpm, denoted as biuret-1000, biuret-3000, and biuret-5000, respectively) and without a biuret buffer layer (reference).

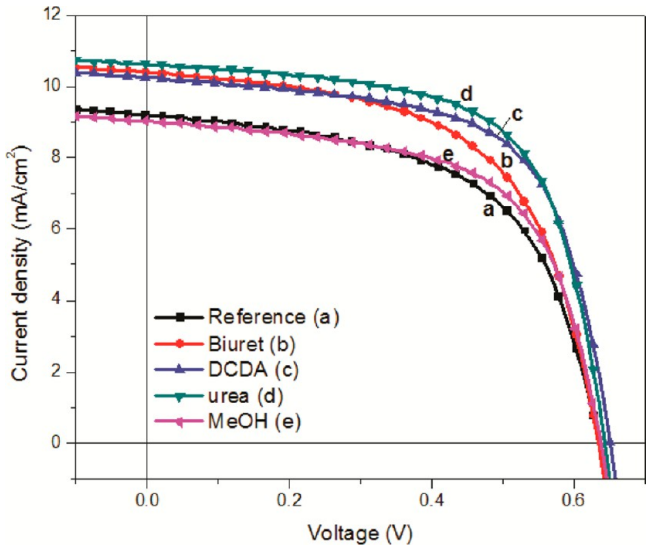

Figure 3. *J*−*V* curves of the ITO/PEDOT:PSS/P3HT:PCBM/CBL/Al BHJ-PSCs with biuret (b), DCDA (c), urea (d), and MeOH (e) CBLs and without any CBL (reference, a).

reference device (curve a). According to the measured photovoltaic parameters (Table 3), PCEs of devices incorporated with CBLs are all dramatically higher than that of the reference P3HT:PCBM device (3.35%), while evidently the enhancement effect is sensitively dependent on the CBL material. In order to unveil the factors responsible for the enhanced PCE with the incorporation of different CBLs, we plotted the dependence of the enhancement ratio of each parameter determining PCE (including V_{oc}, J_{sc}, and FF) on the CBL material in Figure 4. Clearly, V_{oc} of different devices remains almost constant (0.63−0.65 V) compared to that of the reference P3HT:PCBM device, whereas both J_{sc} and FF are obviously higher than that of the reference device: J_{sc} of the CBL-incorporated device increases dramatically by 13%, 11%, and 15% for the cases of biuret, DCDA, and urea, respectively [from 9.21 mA cm^{-2} (reference) to 10.39 mA cm^{-2} (biuret), 10.25 mA cm^{-2} (DCDA), and 10.63 mA cm^{-2} (urea)], while FF values obtained from devices incorporated with biuret, DCDA, and urea are 58%, 63%, and 64%, respectively, all higher than that of the reference device (57%). Consequently, the measured PCEs of devices incorporated with biuret, DCDA, and urea are 3.84%, 4.25%, and 4.39%, respectively, which are enhanced by 15%, 27%, and 31%, respectively, compared to that of the reference device (3.35%). Furthermore, it has been reported that MeOH itself can play a role of CBL, leading to the efficiency enhancement of thieno[3,4-*b*]-thiophene/benzodithiophene (PTB7):[6,6]phenyl-C_{71}-butyric acid methyl ester ($PC_{71}BM$) BHJ-PSC devices with increased built-in voltage owing to passivation of surface traps and an increase in the surface charge density.[47] Thus, for a more accurate evaluation of the effect of our novel CBLs (biuret, DCDA and urea), the influence of MeOH as solvent dissolving the CBL material should be considered. Accordingly, MeOH was spin-coated onto the P3HT:PCBM photoactive layer at the

Table 2. Photovoltaic Parameters of ITO/PEDOT:PSS/P3HT:PCBM/Biuret/Al BHJ-PSCs with Biuret CBLs Prepared at Different Spin-Coating Speeds[a]

device	spin-coating speed (rpm)	V_{oc} (V)	J_{sc} (mA cm^{-2})	FF (%)	PCE (%)	ΔPCE[c] (%)	R_s (Ω cm^2)	R_{sh} (Ω cm^2)
reference[b]		0.64 ± 0.004	9.46 ± 0.16	54 ± 2	3.31 ± 0.12		12.3	350.8
biuret-1000	1000	0.63 ± 0.005	9.47 ± 0.09	58 ± 1	3.45 ± 0.07	4	10.3	503.8
biuret-3000	3000	0.64 ± 0.003	10.11 ± 0.28	58 ± 1	3.72 ± 0.12	13	10.6	464.0
biuret-5000	5000	0.63 ± 0.004	9.45 ± 0.16	59 ± 1	3.51 ± 0.10	6	10.3	549.1

[a]The concentration of a biuret solution in MeOH is fixed at 1.0 mg mL^{-1}. [b]Variation of the PCEs for the reference and biuret-3000 devices compared to those listed in Table 1 is due to the slight difference among different batches of devices and the measurement error. [c]ΔPCE is the enhancement of PCE relative to the reference P3HT:PCBM BHJ-PSCs.

Table 3. Photovoltaic Parameters of the ITO/PEDOT:PSS/P3HT:PCBM/CBL/Al BHJ-PSCs with Different CBLs[a]

device	V_{oc} (V)	J_{sc} (mA cm^{-2})	FF (%)	PCE (%)	ΔPCE[c]	R_s (Ω cm^2)	R_{sh} (Ω cm^2)
reference[b]	0.63 ± 0.005	9.21 ± 0.18	57 ± 2	3.35 ± 0.12		10.3	501.6
biuret	0.63 ± 0.005	10.39 ± 0.28	58 ± 1	3.84 ± 0.12	15	8.7	579.4
DCDA	0.65 ± 0.004	10.25 ± 0.42	63 ± 2	4.25 ± 0.13	27	8.0	647.8
urea	0.64 ± 0.003	10.63 ± 0.27	64 ± 1	4.39 ± 0.14	31	7.5	755.2
MeOH	0.64 ± 0.004	9.02 ± 0.14	61 ± 1	3.53 ± 0.06	5	8.7	620.7

[a]The concentration of the CBL solution in MeOH is fixed at 1.0 mg mL^{-1}, and the spin-coating speed is fixed at 3000 rpm. [b]Variation of the PCEs for the reference and other devices compared to those listed in Tables 1, 2, and S1−S4 in the Supporting Information is due to the slight difference among different batches of devices and the measurement error. [c]ΔPCE is the enhancement of PCE relative to the reference P3HT:PCBM BHJ-PSCs.

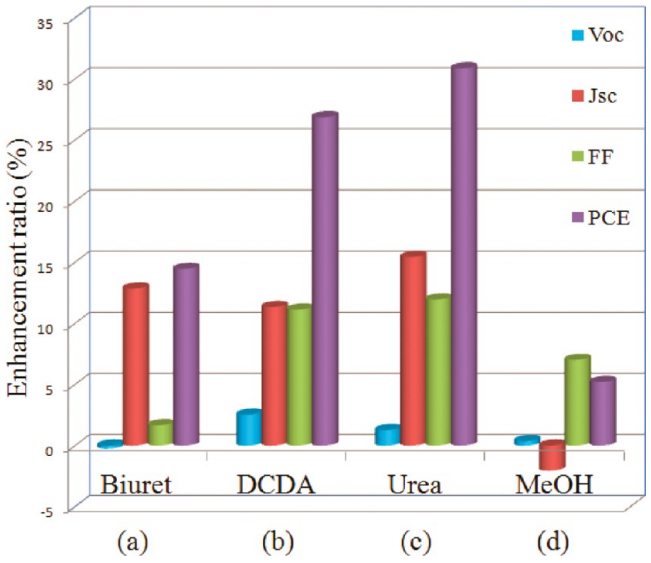

Figure 4. Enhancement ratio of the photovoltaic parameters of P3HT:PCBM BHJ-PSCs with different CBLs of biuret (a), DCDA (b), urea (c), and MeOH (d).

same spin-coating speed (3000 rpm) to that used for CBLs, and the resulting device (curve e) shows only a slight enhancement on PCE (from 3.35% to 3.53%). This result confirms that the efficiency enhancement of CBL-incorporated devices is indeed attributed primarily to the CBL materials (biuret, DCDA and urea).

Surface Morphologies of P3HT:PCBM/CBL Bilayer Films and Thicknesses of CBL Layers. Surface morphologies of the P3HT:PCBM active layer films with and without CBLs were studied by AFM in tapping mode (Figure 5). The surface morphology of the reference P3HT:PCBM film (image a) shows an interpenetrating network of P3HT and PCBM with clear P3HT- and PCBM-rich domains because of their microphase separation behavior, and the film surface is quite smooth with a root-mean-square (RMS) roughness of around 0.8 nm. After the incorporation of CBLs prepared under the optimum spin-coating condition, the domain feature of P3HT:PCBM microphase separation became less discernible, and a negligible difference in the surface morphology and roughness is observed (images b−d), indicating that the CBLs only slightly affect the morphology of the P3HT:PCBM photoactive film. Besides, the surface morphologies of different CBL-incorporated films look quite similar, and this is understandable because the CBL layer is so thin that its influence on the morphology of the underneath P3HT:PCBM active layer is negligible.

Because the rms roughness of the P3HT:PCBM active layer is quite small and expected to be smaller than the thickness of the CBL, it is possible to estimate the thickness of the CBL atop the P3HT:PCBM active layer directly by AFM, which is obtained by subtracting the sum thickness of the PEDOT:PSS/P3HT:PCBM/CBL layer with that of the PEDOT:PSS/P3HT:PCBM layer (see the Supporting Information, Figure S3). Accordingly, the thicknesses of the CBLs are estimated to be 3, 2, and 2 nm for biuret, DCDA, and urea, respectively. With such a small thickness of CBL resulting from the optimized spin-coating condition, the highest efficiency enhancement of the P3HT:PCBM BHJ-PSCs was achieved; otherwise, a thicker CBL prepared from a higher solution concentration or lower spin-coating speed would prohibit electron transport from the active layer to the Al cathode because these CBL materials are insulating, and a thinner CBL would be inferior for its effect on the electron collection as discussed below. In both unoptimized cases, the efficiency enhancement of the P3HT:PCBM BHJ-PSCs upon CBL incorporation is much lower, as revealed above.

Effect of Amino-Containing CBLs on the Efficiency Enhancement of P3HT:PCBM BHJ-PSCs. It is well-known that the electrode materials and the interfaces of donor (acceptor)/electrodes in BHJ-PSC devices are crucial to the charge collection efficiency. Because electron extraction occurs between the interface of the active layer and cathode, ideally the maximum efficiency of electron extraction can be achieved when the work function of the cathode is aligned with the LUMO level of the acceptor in order to form ohmic contact. However, there is an energy level offset (0.3 eV) between the work function of Al (4.3 eV) and the LUMO level of the PCBM acceptor (4.0 eV) (see Scheme 2), resulting in unfavorable electron extraction.[10,17−22] Furthermore, it has been revealed that the strong interaction between Al and the thiophene rings of P3HT may disrupt conjugation of the P3HT main chain, prohibiting efficient hole transport in the donor phase.[48,49] Versatile CBL materials such as LiF, poly(ethylene oxide), poly[(9,9-bis(3′-*N*,*N*-dimethylamino)propyl)-2,7-fluorene]-*alt*-2,7-(9,9-dioctyfluorene)] (PFN), and poly(vinylpyrrolidone) (PVP) have been successfully applied toward optimization of the interface between the PCBM acceptor and Al cathode, and the effect of the CBL was fulfilled through facilitation of electron extraction by means of inducing interfacial charge redistribution, geometry modifications, and/or chemical reactions.[24,25,27−29,34]

As discussed above, the efficiency enhancement with the incorporation of CBLs of biuret, DCDA, and urea is mainly due to the synergetic enhancement of both J_{sc} and FF. Generally, J_{sc} is dependent on not only the multiplication of the photo-induced charge-carrier density and the charge-carrier mobility

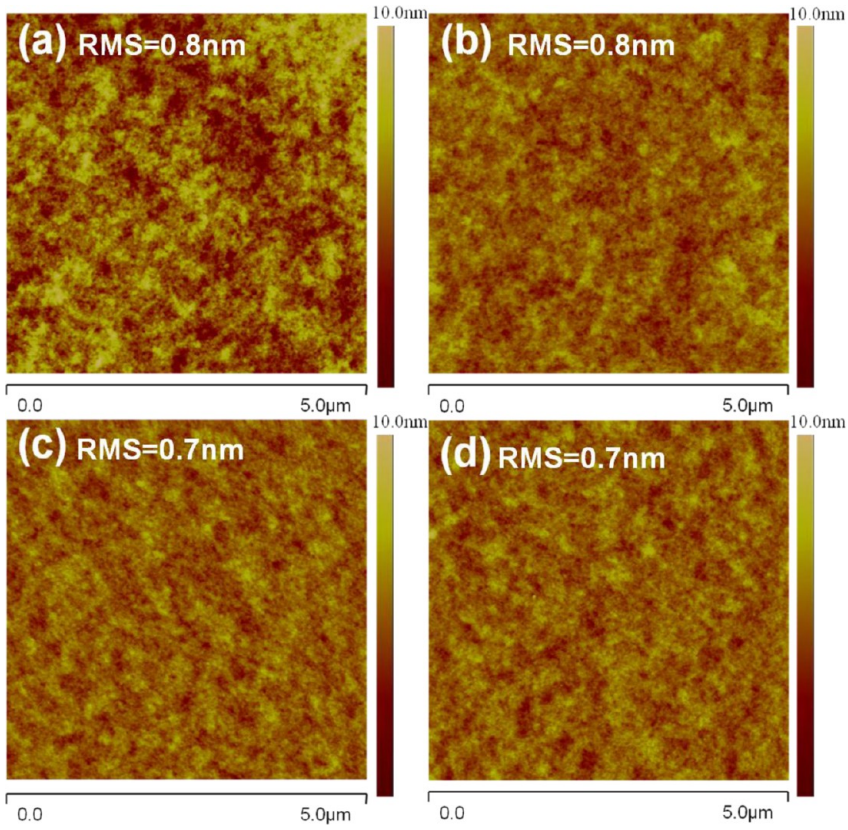

Figure 5. AFM images (5 μm × 5 μm) of P3HT:PCBM photoactive films without CBL (a) and with different CBLs of biuret (b), DCDA (c), and urea (d).

Scheme 2. Energy Level Diagram of ITO/PEDOT:PSS/P3HT:PCBM/CBL/Al BHJ-PSC Devices with the Incorporation of Different CBLs of Biuret, DCDA, and Urea

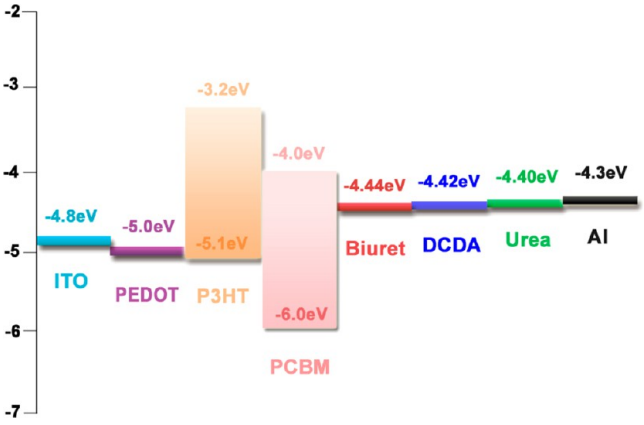

within the active material but also the interface properties between the active layers and electrodes, whereas FF is determined by charge carriers reaching the electrodes, when the built-in field is lowered toward the open-circuit voltage.[1−9,24] Therefore, the enhancement of both J_{sc} and FF upon the incorporation of CBLs might arise from the strong influence of the CBL on the P3HT:PCBM photoactive layer/Al electrode interface. Indeed, the three amino-containing small-molecule organic materials—biuret, DCDA, and urea—have relatively large dipole moments of 3.27, 6.76, and 6.96 D, respectively,[50−52] and this feature makes the formation of a dipole layer via self-assembly possible. Such an assumption was experimentally confirmed by SKPM measurements, which have been recently used to probe an interfacial dipole induced by CBL for BHJ-PSCs and from which the direction of the dipole moment can be simply deduced from the value of the surface potential change upon the incorporation of CBLs.[24,32,34] The surface potential images of P3HT:PCBM active films with and without different CBLs are shown in Figure 6, and the detailed analysis of the surface potential value is given in the Supporting Information, section S3. Clearly, the surface potential over the entire film is uniform for all cases, and the surface potential is sensitively dependent on the CBL material. Compared to the reference P3HT:PCBM active film, which shows a surface potential of 81 mV, the surface potentials of CBL-incorporated films are 158, 183, and 198 mV for biuret, DCDA, and urea, which are 77, 102, and 117 mV more positive than that of the reference P3HT:PCBM film, respectively (see the Supporting Information, section S4). Similar to the cases reported for PFN and PVP as CBLs for BHJ-PSCs, the positive shifts of the surface potential with the incorporation of CBLs (biuret, DCDA, and urea) compared to the reference P3HT:PCBM film suggest that CBLs induce microscopic electric dipole moments for which the positive charge end points toward the Al electrode while the negative charge end points to the P3HT:PCBM layer.[24,32,34] Such CBL-induced dipole moments may decrease effectively the energy level offset between the work function of Al and the LUMO level of the PCBM acceptor, as discussed further below, and consequently lead to an improved P3HT:PCBM photoactive layer/Al electrode interface more favorable for electron extraction. This proposed mechanism is strongly supported by our experimental finding that the synergetic enhancement of both J_{sc} and FF, which are

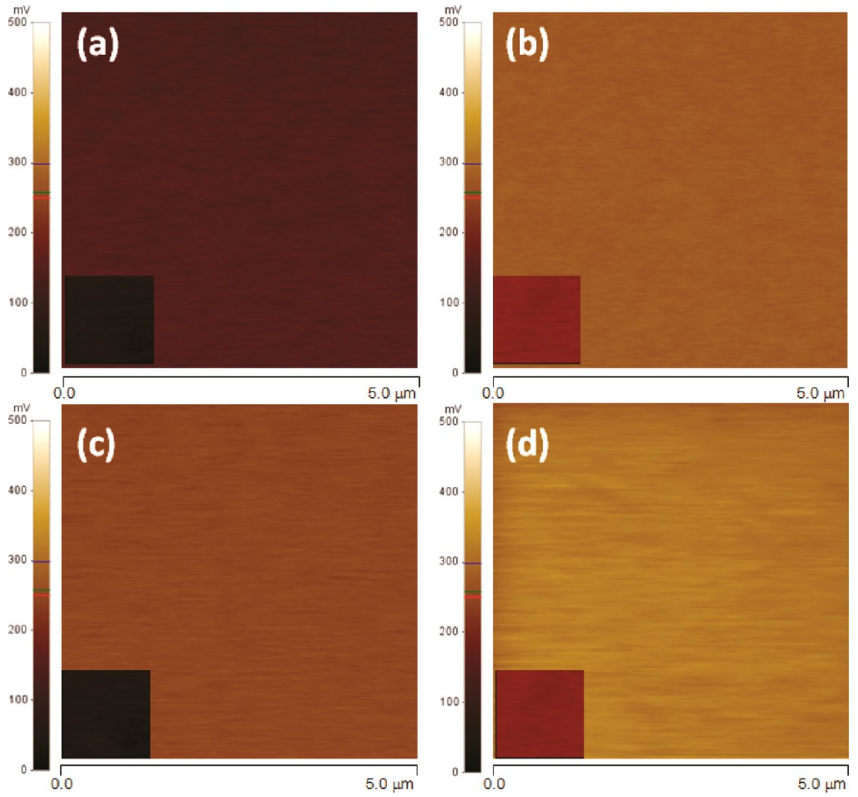

Figure 6. Surface potential images (5 μm × 5 μm) of P3HT:PCBM photoactive films without CBL (a) and with different CBLs of biuret (b), DCDA (c), and urea (d). The inset images (1 μm × 1 μm) are the surface potential images of HOPG, which were measured prior to the sample measurement to ensure accuracy, eliminating the influence of the tip.

sensitively dependent on the P3HT:PCBM photoactive layer/Al electrode interface, primarily contribute to enhancement of the PCE of the CBL-incorporated devices.

In order to understand the difference in the enhancement effect of different CBL materials, we estimated the work functions of biuret, DCDA, and urea based on the surface potential values measured by SKPM.[24,33,53,54] Taking 4.6 eV as the work function of highly oriented pyrolytic graphite (HOPG), which was typically used as the reference of SKPM measurements,[55] the work functions of biuret, DCDA, and urea are estimated to be 4.44, 4.42, and 4.40 eV, respectively (see Scheme 2 and the Supporting Information, section S3). Clearly, among these three CBL materials, the work functions of urea (4.40 eV) and DCDA (4.42 eV) show better matching with that of the P3HT:PCBM reference compared to biuret with a work function of 4.44 eV (see Scheme 2). This result is in good agreement with our experimental finding that the enhancement effects of urea and DCDA CBLs are superior to that of biuret.

For the reference P3HT:PCBM BHJ-PSCs without any CBL, it has been revealed that the strong chemical reaction between Al and the thiophene rings of P3HT may occur, which would disrupt conjugation of the P3HT main chain, prohibiting efficient hole transport in the donor phase.[48,49] Upon the incorporation of amino-containing CBLs of biuret, DCDA, and urea between the P3HT:PCBM active layer and Al cathode, the strong coordination ability of the amino ($-NH_2$) group within the amino-containing CBL materials would lead to the coordination interaction between the lone-pair electrons on the N atoms of the amino group and the Al atoms, thus prohibiting interaction between Al and the thiophene rings of P3HT. Such a protection effect of CBL has been proposed in other CBL materials such as PEG and PVP[34,56,57] and is proposed to partially contribute to the efficiency enhancement of our amino-containing CBL-incorporated devices as well. Thus, the role of the amino group on the performance of biuret, DCDA, and urea as CBLs is revealed, and the different CBL performances of biuret, DCDA, and urea should presumably originate from the differences in their chemical structure, specifically the number of amino groups. Although biuret and urea both have two amino groups, the dipole moment of urea (6.96 D) is much larger than that of biuret (3.27 D),[46,48] facilitating formation of a dipole layer via self-assembly. A further study on the correlation between the molecular structure and CBL performance of such small-molecule organic materials is underway in our laboratories.

CONCLUSIONS

In summary, for the first time we successfully applied three amino-containing small-molecule organic materials including biuret, DCDA, and urea as novel CBLs in P3HT:PCBM BHJ-PSCs via simple spin-coating. Under the optimum solution concentration (1.0 mg mL^{-1} in MeOH) and spin-coating speed (3000 rpm) affording optimum thicknesses of 3, 2, and 2 nm for biuret, DCDA, and urea, respectively, the incorporation of CBLs leads to the dramatic enhancement of the device efficiency by ~15%, ~27%, and ~31% for biuret, DCDA, and urea, respectively. The efficiency enhancement is primarily attributed to the increases of both J_{sc} and FF, suggesting improved electron extraction upon the incorporation of CBLs. The effect of amino-containing CBLs on the efficiency enhancement is interpreted by the conjunct effects of the formation of a dipole layer between the P3HT:PCBM active

dx.doi.org/10.1021/am500013s | ACS Appl. Mater. Interfaces 2014, 6, 4329−4337

layer and Al electrode, which decreases effectively the energy level offset between the work function of Al and the LUMO level of the PCBM acceptor, and the coordination interaction between the lone-pair electrons on the N atoms of the amino group with the Al atoms, which prohibits interaction between Al and the thiophene rings of P3HT. The latter effect may account for the dependence of the CBL performance of biuret, DCDA, and urea on its chemical structure, specifically the number of amino groups. As the first successful and facile application of amino-containing small-molecule organic materials in PSCs, this study provides new insight into the role of the interfacial layer and paves the way for interface engineering in PSCs.

■ ASSOCIATED CONTENT

Supporting Information

Optimization of devices incorporated with DCDA and urea CBLs, determination of the thickness of the CBL, and determination of the work function of the CBL by SKPM. This material is available free of charge via the Internet at http://pubs.acs.org.

■ AUTHOR INFORMATION

Corresponding Author

*E-mail: sfyang@ustc.edu.cn.

Notes

The authors declare no competing financial interest.

■ ACKNOWLEDGMENTS

This work was partially supported by the National Natural Science Foundation of China (Grants 21132007 and 21371164), Key Project of Hefei Center for Physical Science and Technology (Grant 2012FXZY006), and National Basic Research Program of China (Grants 2010CB923300 and 2011CB921400). The work at SINANO was supported by the National Natural Science Foundation of China (Grant 91233104).

■ REFERENCES

(1) Dou, L.; You, J.; Hong, Z.; Xu, Z.; Li, G.; Street, R. A.; Yang, Y. 25th Anniversary Article: A Decade of Organic/Polymeric Photovoltaic Research. *Adv. Mater.* **2013**, *25*, 6642−6671.

(2) Adebanjo, O.; Maharjan, P. P.; Adhikary, P.; Wang, M.; Yang, S.; Qiao, Q. Triple Junction Polymer Solar Cells. *Energy Environ. Sci.* **2013**, *6*, 3150−3170.

(3) Li, G.; Zhu, R.; Yang, Y. Polymer Solar Cells. *Nat. Photonics* **2012**, *6*, 153−161.

(4) Li, Y. Molecular Design of Photovoltaic Materials for Polymer Solar Cells: Toward Suitable Electronic Energy Levels and Broad Absorption. *Acc. Chem. Res.* **2012**, *45*, 723−733.

(5) Chen, W.; Nikiforov, M. P.; Darling, S. B. Morphology Characterization in Organic and Hybrid Solar Cells. *Energy Environ. Sci.* **2012**, *5*, 8045−8074.

(6) Cai, W.; Gong, X.; Cao, Y. Polymer Solar Cells: Recent Development and Possible Routes for Improvement in the Performance. *Sol. Energy Mater. Sol. Cells* **2010**, *94*, 114−127.

(7) Krebs, F. C.; Fyenbo, J.; Jørgensen, M. Product Integration of Compact Roll-to-Roll Processed Polymer Solar Cell Modules: Methods and Manufacture Using Flexographic Printing, Slot-Die Coating and Rotary Screen Printing. *J. Mater. Chem.* **2010**, *20*, 8994−9001.

(8) Deibel, C.; Dyakonov, V. Polymer−Fullerene Bulk Heterojunction Solar Cells. *Rep. Prog. Phys.* **2010**, *73*, 096401.

(9) Dennler, G.; Scharber, M. C.; Brabec, C. J. Polymer−Fullerene Bulk-Heterojunction Solar Cells. *Adv. Mater.* **2009**, *21*, 1323−1338.

(10) Dang, M. T.; Hirsch, L.; Wantz, G. P3HT:PCBM, Best Seller in Polymer Photovoltaic Research. *Adv. Mater.* **2011**, *23*, 3597−3602.

(11) Dang, M. T.; Hirsch, L.; Wantz, G.; Wuest, J. D. Controlling the Morphology and Performance of Bulk Heterojunctions in Solar Cells. Lessons Learned from the Benchmark Poly(3-Hexylthiophene):[6,6]-Phenyl-C61-Butyric Acid Methyl Ester System. *Chem. Rev.* **2013**, *113*, 3734−3765.

(12) Liao, S. H.; Jhuo, H. J.; Cheng, Y. S.; Chen, S. A. Fullerene Derivative-Doped Zinc Oxide Nanofilm as the Cathode of Inverted Polymer Solar Cells with Low-Bandgap Polymer (PTB7-Th) for High Performance. *Adv. Mater.* **2013**, *25*, 4766−4771.

(13) You, J.; Dou, L.; Yoshimura, K.; Kato, T.; Ohya, K.; Moriarty, T.; Emery, K.; Chen, C.-C.; Gao, J.; Li, G. A Polymer Tandem Solar Cell with 10.6% Power Conversion Efficiency. *Nat. Commun.* **2013**, *4*, 1446.

(14) He, Z.; Zhong, C.; Su, S.; Xu, M.; Wu, H.; Cao, Y. Enhanced Power-Conversion Efficiency in Polymer Solar Cells Using an Inverted Device Structure. *Nat. Photonics* **2012**, *6*, 591−595.

(15) Moulé, A. J.; Meerholz, K. Controlling Morphology in Polymer−Fullerene Mixtures. *Adv. Mater.* **2008**, *20*, 240−245.

(16) Zhang, F.; Jespersen, K. G.; Björström, C.; Svensson, M.; Andersson, M. R.; Sundström, V.; Magnusson, K.; Moons, E.; Yartsev, A.; Inganäs, O. Influence of Solvent Mixing on the Morphology and Performance of Solar Cells Based on Polyfluorene Copolymer/Fullerene Blends. *Adv. Funct. Mater.* **2006**, *16*, 667−674.

(17) Chen, L.-M.; Xu, Z.; Hong, Z.; Yang, Y. Interface Investigation and Engineering—Achieving High Performance Polymer Photovoltaic Devices. *J. Mater. Chem.* **2010**, *20*, 2575−2598.

(18) Ma, H.; Yip, H.-L.; Huang, F.; Jen, A. K. Y. Interface Engineering for Organic Electronics. *Adv. Funct. Mater.* **2010**, *20*, 1371−1388.

(19) Po, R.; Carbonera, C.; Bernardi, A.; Camaioni, N. The Role of Buffer Layers in Polymer Solar Cells. *Energy Environ. Sci.* **2011**, *4*, 285−310.

(20) Steim, R.; Kogler, F. R.; Brabec, C. J. Interface Materials for Organic Solar Cells. *J. Mater. Chem.* **2010**, *20*, 2499−2512.

(21) Yip, H.-L.; Jen, A. K. Y. Recent Advances in Solution-Processed Interfacial Materials for Efficient and Stable Polymer Solar Cells. *Energy Environ. Sci.* **2012**, *5*, 5994−6011.

(22) Chen, F.; Chen, Q.; Mao, L.; Wang, Y.; Huang, X.; Lu, W.; Wang, B.; Chen, L. Tuning Indium Tin Oxide Work Function with Solution-Processed Alkali Carbonate Interfacial Layers for High-Efficiency Inverted Organic Photovoltaic Cells. *Nanotechnology* **2013**, *24*, 484011.

(23) Gupta, V.; Kyaw, A. K.; Wang, D. H.; Chand, S.; Bazan, G. C.; Heeger, A. J. Barium: An Efficient Cathode Layer for Bulk-Heterojunction Solar Cells. *Sci. Rep.* **2013**, *3*, 1965.

(24) He, Z.; Zhong, C.; Huang, X.; Wong, W. Y.; Wu, H.; Chen, L.; Su, S.; Cao, Y. Simultaneous Enhancement of Open-Circuit Voltage, Short-Circuit Current Density, and Fill Factor in Polymer Solar Cells. *Adv. Mater.* **2011**, *23*, 4636−4643.

(25) Li, J.; Huang, X.; Yuan, J.; Lu, K.; Yue, W.; Ma, W. A New Alcohol-Soluble Electron-Transporting Molecule for Efficient Inverted Polymer Solar Cells. *Org. Electron.* **2013**, *14*, 2164−2171.

(26) Liu, F.; Page, Z. A.; Duzhko, V. V.; Russell, T. P.; Emrick, T. Conjugated Polymeric Zwitterions as Efficient Interlayers in Organic Solar Cells. *Adv. Mater.* **2013**, *25*, 6868−6873.

(27) Zhang, F.; Ceder, M.; Inganäs, O. Enhancing the Photovoltage of Polymer Solar Cells by Using a Modified Cathode. *Adv. Mater.* **2007**, *19*, 1835−1838.

(28) Brabec, C. J.; Shaheen, S. E.; Winder, C.; Sariciftci, N. S.; Denk, P. Effect of LiF/Metal Electrodes on the Performance of Plastic Solar Cells. *Appl. Phys. Lett.* **2002**, *80*, 1288−1290.

(29) Chen, X.; Zhao, C.; Rothberg, L.; Ng, M.-K. Plasmon Enhancement of Bulk Heterojunction Organic Photovoltaic Devices by Electrode Modification. *Appl. Phys. Lett.* **2008**, *93*, 123302.

(30) Kim, J. Y.; Kim, S. H.; Lee, H. H.; Lee, K.; Ma, W.; Gong, X.; Heeger, A. J. New Architecture for High-Efficiency Polymer

Photovoltaic Cells Using Solution-Based Titanium Oxide as an Optical Spacer. *Adv. Mater.* **2006**, *18*, 572−576.
(31) Kim, J. Y.; Lee, K.; Coates, N. E.; Moses, D.; Nguyen, T. Q.; Dante, M.; Heeger, A. J. Efficient Tandem Polymer Solar Cells Fabricated by All-Solution Processing. *Science* **2007**, *317*, 222−225.
(32) Zhang, W.; Wang, H.; Chen, B.; Bi, X.; Venkatesan, S.; Qiao, Q.; Yang, S. Oleamide as a Self-Assembled Cathode Buffer Layer for Polymer Solar Cells: The Role of the Terminal Group on the Function of the Surfactant. *J. Mater. Chem.* **2012**, *22*, 24067−24074.
(33) Lv, M.; Li, S.; Jasieniak, J. J.; Hou, J.; Zhu, J.; Tan, Z.; Watkins, S. E.; Li, Y.; Chen, X. A Hyperbranched Conjugated Polymer as the Cathode Interlayer for High-Performance Polymer Solar Cells. *Adv. Mater.* **2013**, *25*, 6889−6894.
(34) Wang, H.; Zhang, W.; Xu, C.; Bi, X.; Chen, B.; Yang, S. Efficiency Enhancement of Polymer Solar Cells by Applying Poly(Vinylpyrrolidone) as a Cathode Buffer Layer via Spin Coating or Self-Assembly. *ACS Appl. Mater. Interfaces* **2013**, *5*, 26−34.
(35) Du, H.; Deng, Z.; Lü, Z.; Chen, Z.; Zou, Y.; Yin, Y.; Xu, D.; Wang, Y. The Effect of Small-Molecule Electron Transporting Materials on the Performance of Polymer Solar Cells. *Thin Solid Films* **2011**, *519*, 4357−4360.
(36) Tan, Z.; Zhang, W.; Zhang, Z.; Qian, D.; Huang, Y.; Hou, J.; Li, Y. High-Performance Inverted Polymer Solar Cells with Solution-Processed Titanium Chelate as Electron-Collecting Layer on ITO Electrode. *Adv. Mater.* **2012**, *24*, 1476−1481.
(37) Tan, Z.; Yang, C.; Zhou, E.; Wang, X.; Li, Y. Performance Improvement of Polymer Solar Cells by Using a Solution Processible Titanium Chelate as Cathode Buffer Layer. *Appl. Phys. Lett.* **2007**, *91*, 023509.
(38) Li, S.; Lei, M.; Lv, M.; Watkins, S. E.; Tan, Z.; Zhu, J.; Hou, J.; Chen, X.; Li, Y. [6,6]-Phenyl-C61-Butyric Acid Dimethylamino Ester as a Cathode Buffer Layer for High-Performance Polymer Solar Cells. *Adv. Energy Mater.* **2013**, *3*, 1569−1574.
(39) Zhang, Z.-G.; Li, H.; Qi, B.; Chi, D.; Jin, Z.; Qi, Z.; Hou, J.; Li, Y.; Wang, J. Amine Group Functionalized Fullerene Derivatives as Cathode Buffer Layers for High Performance Polymer Solar Cells. *J. Mater. Chem. A* **2013**, *1*, 9624−9629.
(40) Chen, B.; Zhang, W.; Zhou, X.; Huang, X.; Zhao, X.; Wang, H.; Liu, M.; Lu, Y.; Yang, S. Surface Plasmon Enhancement of Polymer Solar Cells by Penetrating Au/SiO_2 Core/Shell Nanoparticles into All Organic Layers. *Nano Energy* **2013**, *2*, 906−915.
(41) Chen, M.; Li, M.; Wang, H.; Qu, S.; Zhao, X.; Xie, L.; Yang, S. Side-Chain Substitution of Poly(3-Hexylthiophene) (P3HT) by PCBM via Postpolymerization: An Intramolecular Hybrid of Donor and Acceptor. *Polym. Chem.* **2013**, *4*, 550−557.
(42) Qu, S.; Li, M.; Xie, L.; Huang, X.; Yang, J.; Wang, N.; Yang, S. Noncovalent Functionalization of Graphene Attaching [6,6]-Phenyl-C61-Butyric Acid Methyl Ester (PCBM) and Application as Electron Extraction Layer of Polymer Solar Cells. *ACS Nano* **2013**, *7*, 4070−4081.
(43) Zhang, W.; Xu, Y.; Wang, H.; Xu, C.; Yang, S. Fe_3O_4 Nanoparticles Induced Magnetic Field Effect on Efficiency Enhancement of P3HT:PCBM Bulk Heterojunction Polymer Solar Cells. *Sol. Energy Mater. Sol. Cells* **2011**, *95*, 2880−2885.
(44) Zhang, W.; Zhao, B.; He, Z.; Zhao, X.; Wang, H.; Yang, S.; Wu, H.; Cao, Y. High-Efficiency ITO-Free Polymer Solar Cells Using Highly Conductive PEDOT:PSS/Surfactant Bilayer Transparent Anodes. *Energy Environ. Sci.* **2013**, *6*, 1956−1964.
(45) Zhang, Z.-G.; Li, H.; Qi, Z.; Jin, Z.; Liu, G.; Hou, J.; Li, Y.; Wang, J. Poly(Ethylene Glycol) Modified [60]Fullerene as Electron Buffer Layer for High-Performance Polymer Solar Cells. *Appl. Phys. Lett.* **2013**, *102*, 143902.
(46) Sun, K.; Zhao, B.; Murugesan, V.; Kumar, A.; Zeng, K.; Subbiah, J.; Wong, W. W. H.; Jones, D. J.; Ouyang, J. High-Performance Polymer Solar Cells with a Conjugated Zwitterion by Solution Processing or Thermal Deposition as the Electron-Collection Interlayer. *J. Mater. Chem.* **2012**, *22*, 24155−24165.
(47) Zhou, H.; Zhang, Y.; Seifter, J.; Collins, S. D.; Luo, C.; Bazan, G. C.; Nguyen, T.-Q.; Heeger, A. J. High-Efficiency Polymer Solar Cells Enhanced by Solvent Treatment. *Adv. Mater.* **2013**, *25*, 1646−1652.
(48) Dannetun, P.; Boman, M.; Stafström, S.; Salaneck, W. R.; Lazzaroni, R.; Fredriksson, C.; Brédas, J. L.; Zamboni, R.; Taliani, C. The Chemical and Electronic Structure of the Interface Between Aluminum and Polythiophene Semiconductors. *J. Chem. Phys.* **1993**, *99*, 664−772.
(49) Salaneck, W. R.; Brédas, J. L. The Metal-on-Polymer Interface in Polymer Light Emitting Diodes. *Adv. Mater.* **1996**, *8*, 48−52.
(50) Kumler, W. D.; Lee, C. M. The Dipole Moment and Structure of Biuret. *J. Am. Chem. Soc.* **1960**, *82*, 6305−6306.
(51) Hirshfeld, F. L.; Hope, H. An X-Ray Determination of the Charge Deformation Density in 2-Cyanoguanidine. *Acta Crystallogr., Sect. B: Struct. Crystallogr. Cryst. Chem.* **1980**, *36*, 406−415.
(52) Birkedal, H.; Madsen, D.; Mathiesen, R. H.; Knudsen, K.; Weber, H. P.; Pattison, P.; Schwarzenbach, D. The Charge Density of Urea from Synchrotron Diffraction Data. *Acta Crystallogr., Sect. A: Found. Crystallogr.* **2004**, *60*, 371−381.
(53) Melitz, W.; Shen, J.; Kummel, A. C.; Lee, S. Kelvin Probe Force Microscopy and Its Application. *Surf. Sci. Rep.* **2011**, *66*, 1−27.
(54) Siddiki, M. K.; Venkatesan, S.; Galipeau, D.; Qiao, Q. Kelvin Probe Force Microscopic Imaging of the Energy Barrier and Energetically Favorable Offset of Interfaces in Double-Junction Organic Solar Cells. *ACS Appl. Mater. Interfaces* **2013**, *5*, 1279−1286.
(55) Palma, M.; Levin, J.; Lemaur, V.; Liscio, A.; Palermo, V.; Cornil, J.; Geerts, Y.; Lehmann, M.; Samorì, P. Self-Organization and Nanoscale Electronic Properties of Azatriphenylene-Based Architectures: A Scanning Probe Microscopy Study. *Adv. Mater.* **2006**, *18*, 3313−3317.
(56) Chen, F.-C.; Chien, S.-C. Nanoscale Functional Interlayers Formed Through Spontaneous Vertical Phase Separation in Polymer Photovoltaic Devices. *J. Mater. Chem.* **2009**, *19*, 6865−6869.
(57) Deng, X. Y.; Lau, W. M.; Wong, K. Y.; Low, K. H.; Chow, H. F.; Cao, Y. High Efficiency Low Operating Voltage Polymer Light-Emitting Diodes With Aluminum Cathode. *Appl. Phys. Lett.* **2004**, *84*, 3522−3524.